UNDERSTANDING ENSO DIVERSITY

BY ANTONIETTA CAPOTONDI, ANDREW T. WITTENBERG, MATTHEW NEWMAN, EMANUELE DI LORENZO, JIN-YI YU, PASCALE BRACONNOT, JULIA COLE, BORIS DEWITTE, BENJAMIN GIESE, ERIC GUILYARDI, FEI-FEI JIN, KRISTOPHER KARNAUSKAS, BENJAMIN KIRTMAN, TONG LEE, NIKLAS SCHNEIDER, YAN XUE, AND SANG-WOOK YEH

Improved determination of ENSO predictability, teleconnections, and impacts requires a better understanding of event-to-event differences in ENSO spatial patterns and evolution.

El Niño–Southern Oscillation (ENSO) is a naturally occurring phenomenon in the tropical Pacific that has global impacts of great relevance to society. The term *El Niño* refers to warming of the tropical Pacific Ocean occurring every 2–7 yr, while the opposite cold phase is known as La Niña. Anomalous warming or cooling conditions are associated with a large-scale east–west sea level pressure seesaw, termed the Southern Oscillation, which represents the atmospheric manifestation of the coupled ENSO phenomenon (McPhaden et al. 2006). ENSO events differ in amplitude, temporal evolution, and spatial pattern. While differences among ENSO events have been known for many years, a renewed interest in this diversity was stimulated by Larkin and Harrison (2005) and Ashok et al. (2007), who highlighted an unusual sea surface temperature anomaly (SSTA) pattern over the tropical Pacific during the summer of 2004 that was associated with remote impacts on surface air temperature and precipitation different from those related to "typical" El Niño conditions. Because of the similarity and differences from a typical El Niño, Ashok et al. (2007) named this pattern El Niño Modoki (a Japanese word that means similar but different) and argued that it is a different type of El Niño. Significant research has since been conducted to identify, describe, and understand these "El Niño types," spurring debates on whether there are indeed two distinct modes of variability, or whether ENSO can be more aptly described as a diverse continuum. In this article, we report on advances in understanding ENSO diversity, drawing from community discussions that took place at the U.S. CLIVAR ENSO Diversity Workshop held in Boulder, Colorado,

AFFILIATIONS: CAPOTONDI AND NEWMAN—University of Colorado Boulder, and NOAA/Earth System Research Laboratory, Boulder, Colorado; WITTENBERG—NOAA/Geophysical Fluid Dynamics Laboratory, Princeton, New Jersey; DI LORENZO—Georgia Institute of Technology, Atlanta, Georgia; YU—University of California, Irvine, Irvine, California; BRACONNOT—Laboratoire des Sciences du Climat et de l'Environnement, Gif-sur-Yvette, France; COLE—The University of Arizona, Tucson, Arizona; DEWITTE—LEGOS, Toulouse, France; GIESE—Texas A&M, College Station, Texas; GUILYARDI—LOCEAN/IPSL, Paris, France, and University of Reading, Reading, United Kingdom; JIN AND SCHNEIDER—University of Hawai'i at Mānoa, Honolulu, Hawaii; KARNAUSKAS—Woods Hole Oceanographic Institution, Woods Hole, Massachusetts; KIRTMAN—University of Miami, Miami, Florida; LEE—Jet Propulsion Laboratory, California Institute of Technology, Pasadena, California; XUE—Climate Prediction Center, College Park, Maryland; YEH—Hanyang University, Ansan, South Korea

CORRESPONDING AUTHOR: Antonietta Capotondi, NOAA/ESRL/PSD1, 325 Broadway, Boulder, CO 80305
E-mail: antonietta.capotondi@noaa.gov

The abstract for this article can be found in this issue, following the table of contents.

DOI:10.1175/BAMS-D-13-00117.1

In final form 8 September 2014
©2015 American Meteorological Society

Unauthenticated | Downloaded 12/18/20 10:22 AM UTC

during 6–8 February 2013 (U.S.CLIVAR ENSO Diversity Working Group 2013).

WHAT IS "ENSO DIVERSITY"? A common way to highlight ENSO diversity is to contrast SSTA patterns at the height of different ENSO events. Figure 1 (right) shows boreal winter SSTAs for the 1997/98 and 2004/05 El Niños, as well as the 2007/08 and 1988/89 La Niñas. For 1997/98, SSTAs peak along the western coast of South America, and extend westward along the equator with decreasing amplitude—a pattern similar to the "canonical" El Niño described by Rasmusson and Carpenter (1982). For 2004/05, on the other hand, the positive SSTAs are substantially weaker, and peak near the date line, with no significant warming of the east Pacific cold tongue region. La Niña events, which tend to peak farther west than warm events, show subtler interevent differences in their spatial patterns. For this reason, most of the emphasis in ENSO diversity research has been devoted to warm events. Several indices have been introduced to characterize the differences in the spatial patterns of El Niño and their associated surface and subsurface characteristics (see sidebar "Indices of El Niño diversity"). In the following, we will refer to events resembling the 1997/98 and 2004/05 cases as eastern Pacific (EP) and central Pacific (CP) El Niños, respectively, following Kao and Yu (2009). Note, however, that in this paper these definitions are used as shorthand for a qualitative description, and do not imply a clear dichotomy between EP and CP event types. In fact, when examining the distribution of events in longitude–amplitude phase space (Fig. 1, left) we see that both warm and cold events occur over a broad range of longitudes. While some of the events that we define as EP and CP capture the extrema of that distribution, there are also many events that comingle in the center. For

INDICES OF EL NIÑO DIVERSITY

To better understand ENSO diversity, several indices have been introduced to identify different event types, with emphasis on the warm (El Niño) ENSO phase. Indices have been constructed from SST (indices a–d), subsurface ocean temperature (index e), sea surface salinity (index f), or outgoing longwave radiation anomaly information (index g). Definitions of El Niño types often vary with the method used.

a) *Niño-3–4 index method (Kug et al. 2009; Yeh et al. 2009):* An El Niño event is classified as a "warm pool" type if its SSTA averaged over the Niño-4 region (5°–5°N, 160°E–150°W) exceeds one standard deviation, and exceeds the SSTA averaged over the Niño-3 region (5°–5°N, 90°–150°W). "Cold tongue" events are characterized by Niño-3 SSTA exceeding one standard deviation, and exceeding the Niño-4 SSTA.
b) *El Niño Modoki index (EMI) method (Ashok et al. 2007):* This index is constructed as the difference between SSTA averaged over the central Pacific (10°S–10°N, 165°E–140°W) and SSTA averaged over the western (10°S–20°N, 125°–145°E) and eastern (15°S–5°N, 110°–70°W) Pacific, to emphasize the out-of-phase relationship between SSTA in the central Pacific versus the eastern–western Pacific.
c) *EP–CP index method (Kao and Yu 2009; Yu et al. 2012):* Regression of SSTA onto the Niño-1+2 index (average SSTA over the region 0°–10°S, 90°–80°W) is used to remove the SSTA component associated with east Pacific warming, and then a principal components analysis (PCA) is used to determine the spatial pattern and associated temporal index of the CP events. Similarly, regression of SSTA onto the Niño-4 index is used to remove the SSTA component associated with central Pacific warming, and then PCA is used to determine the pattern and index of the EP events. A related approach uses the Niño-3 index to identify EP events and also employs the leading principal component of tropical Pacific SSTA (after removal of the SSTA regression onto the Niño-3 index) to identify central Pacific warming (CPW) events (Di Lorenzo et al. 2010).
d) *E and C indices (Takahashi et al. 2011):* This method uses two orthogonal axes that are rotated 45° relative to the principal components of SSTA in the tropical Pacific. The associated projections of the SSTA onto these rotated axes provide the E-index (representing the eastern Pacific El Niño) and the C-index (representing both the central Pacific El Niño and La Niña events).
e) *EP–CP subsurface index method (Yu et al. 2011):* CP El Niños produce their largest subsurface temperature anomalies in the central Pacific, where EP El Niños exhibit only weak subsurface anomalies. With this method, temperature anomalies for the top 100 m of the ocean are averaged over the eastern and central equatorial Pacific to construct EP and CP indices, respectively.
f) *Sea surface salinity (SSS) index method (Singh et al. 2011; Qu and Yu 2014):* SSS anomaly distributions differ among different El Niño events. SSS indices were defined utilizing these differences in the western-to-central equatorial Pacific (Singh et al. 2011) and in the southeastern Pacific (Qu and Yu 2014) to distinguish El Niño types.
g) *Outgoing longwave radiation (OLR) index method (Chiodi and Harrison 2013):* An index was constructed using OLR anomalies over the eastern-to-central equatorial Pacific, to separate events into El Niños characterized by an OLR signal and those without an OLR signal. The two classes of events so identified were found to produce different remote climate impacts.

Unauthenticated | Downloaded 12/18/20 10:22 AM UTC

these events, their identification as EP or CP depends somewhat on the methodology used. Notice that the strongest events occur in the eastern Pacific, with El Niños having potentially larger amplitudes than La Niñas. In the central Pacific, on the other hand, negative events tend to be a little stronger than positive events. This amplitude asymmetry between positive and negative events, which is itself a function of longitude, may be an indication of nonlinearities in the system (Takahashi et al. 2011; Dommenget et al. 2013; Choi et al. 2013; Graham et al. 2014), and represents another important aspect of ENSO diversity.

Differences in the location and strength of the SSTA maximum correspond to differences in the evolution of each ENSO event. For example, Fig. 2 hows how SSTA patterns similar to EP and CP cases (Fig. 2, middle) evolve from some initial tropical anomaly pattern, or "precursor," as shown in the top panels of Fig. 2. In this example, the precursor patterns have been determined from observed SSTs, 20°C isotherm depth, and zonal surface wind stress over the period 1959–2000, by fitting a linear stochastically forced dynamical model to the observations (Penland and Sardeshmukh 1995; Newman et al.

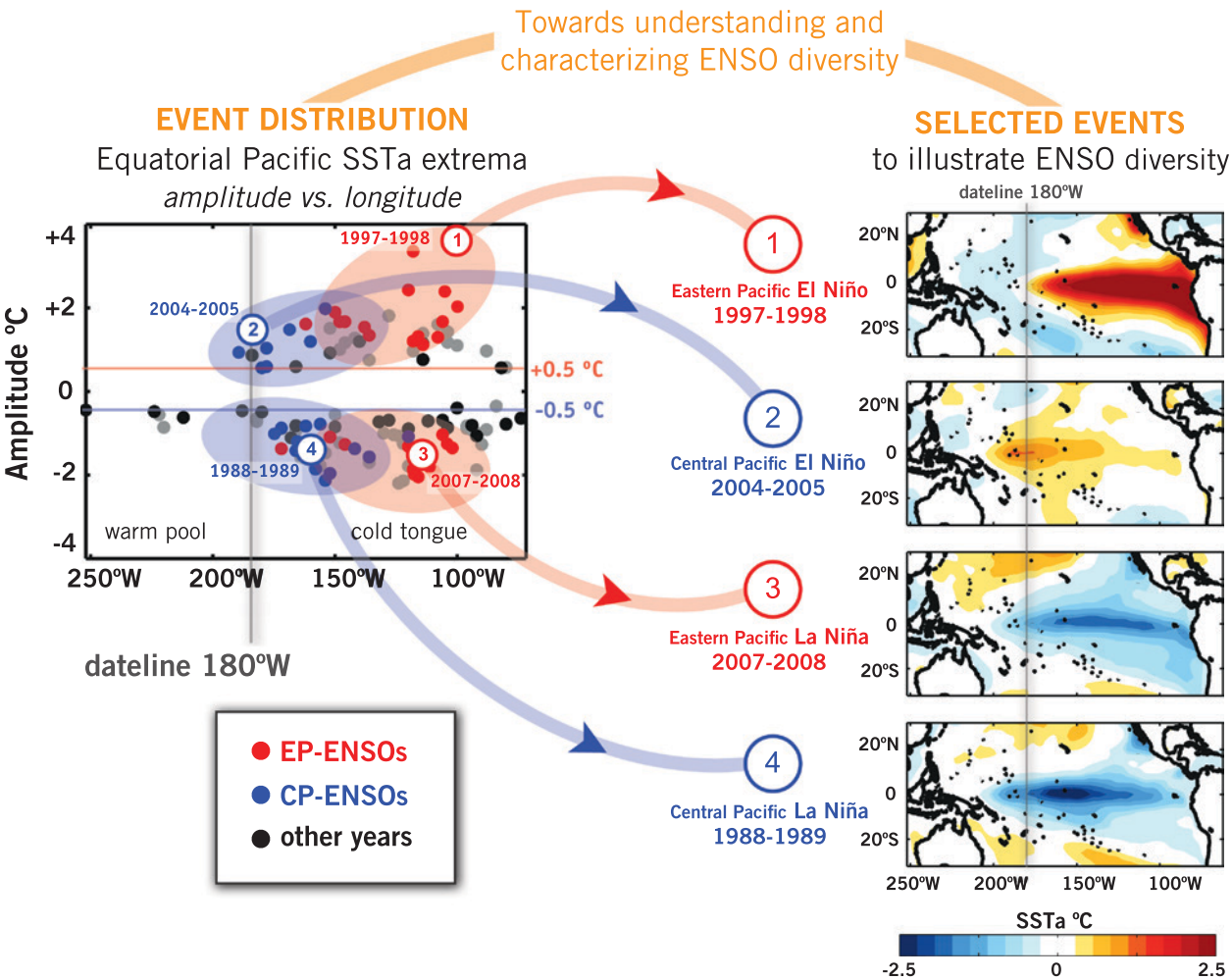

Fig. 1. (left) Distribution of boreal winter [Nov–Jan (NDJ)] SSTA extrema in the longitude–amplitude plane. Anomalies were obtained from the National Oceanic and Atmospheric Administration (NOAA) extended reconstructed SST dataset (Smith and Reynolds 2004) over the period 1900–2013, as departures from the 1945–2013 climatology. Each dot corresponds to the extreme positive or negative value over the NDJ of each year in the region 2°S–2°N, 110°E–90°W. Events prior to 1945 are colored in gray. Events after 1945 are considered EP (red dots) when the Niño-3 index exceeds one standard deviation. CP events are identified using the leading principal component of the SSTA residual after removing the SSTA regression onto the Niño-3 index. Blue dots in the left panel correspond to events for which the leading principal component (used as CP index) exceeds one standard deviation. (right) The spatial patterns of SSTA for specific warm and cold events of either type are shown, with a contour interval of 0.25°C.

Unauthenticated | Downloaded 12/18/20 10:22 AM UTC

2011a,b). Observed anomalies that have a large projection on one of the precursor structures at some given time also have a large projection on the corresponding evolved structure 6 months later (Fig. 2, bottom). However, within this framework, in general ENSO events are neither solely CP nor EP events, but rather different linear combinations of both of these ENSO flavors (color shading in bottom panels of Fig. 2), which themselves result from different balances of physical processes. Some nonlinear processes, not fully captured by the above linear stochastic model, may also play an important role in the evolution of strong events, either EP El Niño or CP La Niña (Jin et al. 2003; Takahashi et al. 2011; Choi et al. 2013; Vecchi et al. 2006), and may differentiate their evolution from weaker events. The EP and CP cases also have different seasonal patterns of evolution (Kao and Yu 2009; Yeh et al. 2014). For EP events, SSTAs typically appear in the far eastern Pacific during spring and extend westward during summer and fall, while in the CP cases anomalies extend from the eastern subtropics to the central Pacific during spring and summer. Both event types achieve their maximum amplitude during boreal winter. The exact onset

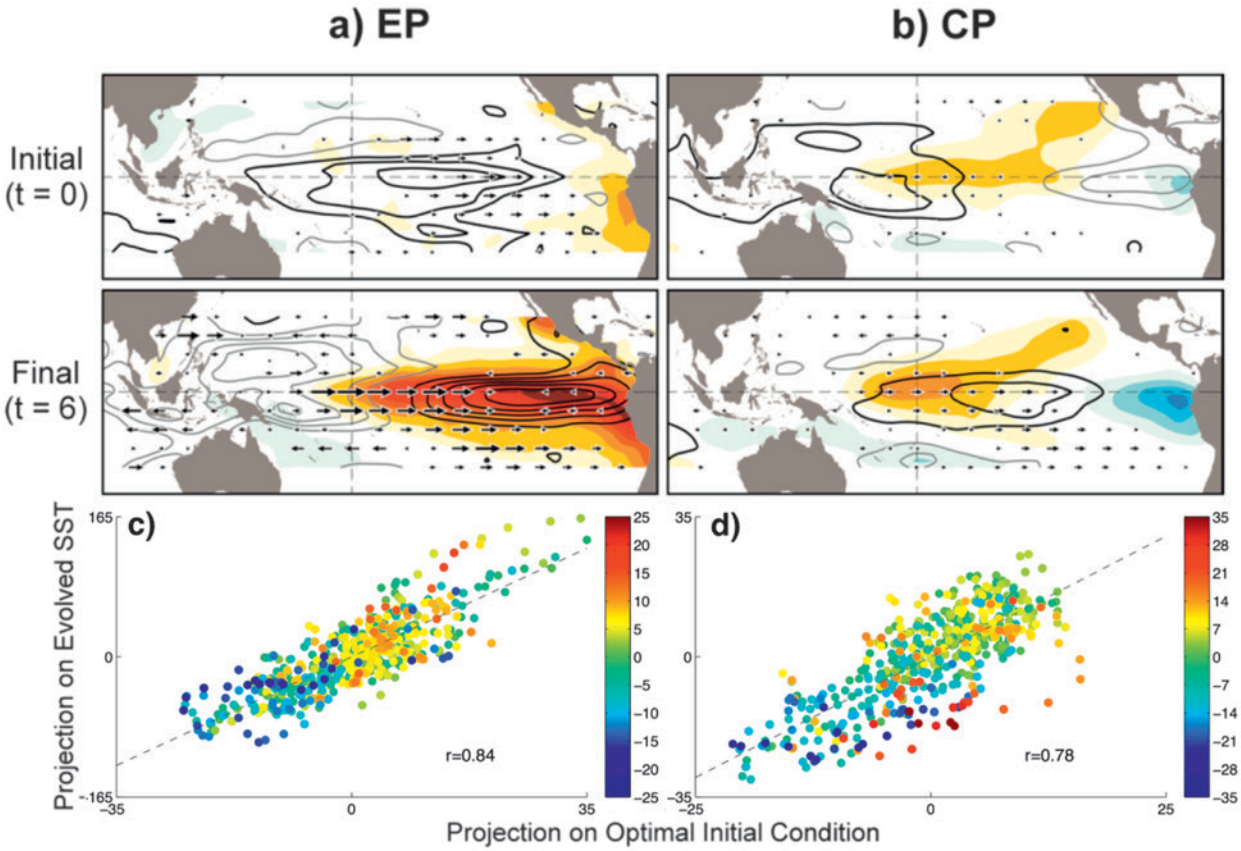

Fig. 2. Evolution of SSTAs from (top) the initial conditions to (middle) the final states 6 months later. The initial conditions (i.e., optimal structures) are obtained by determining a linear stochastically forced dynamical model from SSTAs [HadISST dataset; Rayner et al. (2003)], thermocline depth anomalies [SODA dataset; Carton and Giese (2008)], and zonal wind stress anomalies [National Centers for Environmental Prediction (NCEP)–NCAR reanalysis; Kalnay et al. (1996)], over the period 1959–2000. (a) Evolution of the first pattern (which leads to an EP-type ENSO) shown as maps at *t* = (top) 0 and (middle) 6 months. (b) As in (a), but for the evolution of the second pattern (which leads to a CP-type ENSO). Anomalous SST is indicated by shading (contour interval is 0.25 K), thermocline depth by contours (contour interval is 5 m, where black is positive), and zonal wind stress by black vectors (scaled by the reference vector 0.02 N m^{-2}, with values below 0.002 N m^{-2} removed for clarity). Note that within this linear framework, the opposite-signed patterns lead to cold events. (bottom) Projection of observations onto the optimal initial conditions for SST anomaly amplification over a 6-month interval vs the projection onto the optimal evolved SST state 6 months later, for the (c) EP and (d) CP patterns. Note that the tropical SST growth factor (indicated by the range of the ordinate) for the EP pattern is almost 4 times greater than for the CP pattern. Color shading of dots in the EP (CP) panel indicates the value of the projection on the CP (EP) optimal initial conditions. [Adapted from Newman et al. (2011b).]

Unauthenticated | Downloaded 12/18/20 10:22 AM UTC

and evolution of individual events of either type is somewhat dependent on the timing and strength of the high-frequency atmospheric forcing that trigger each event (Karnauskas 2013), as further discussed in the "Predictability and Prediction" section.

Understanding ENSO diversity has been hampered by the relatively short duration of the observational record. Marine observations are very sparse for most of the twentieth century, with a large increase over the last 30 years (Yu and Giese 2013). Attempts have been made to extend the observational record back in time via "reconstruction" techniques, which often use spatial patterns typical of recent observationally dense periods as basis functions, to project SSTAs into earlier periods with sparse observations. Because these reconstructions [i.e., the Hadley Centre Sea Ice and Sea Surface Temperature dataset (HadISST), the extended reconstructed SST dataset (ERSST), the Kaplan dataset] rely primarily on the spatial structure of ENSO over the last 30 years, ENSO events in these reconstructions may be biased toward the patterns of recent events, leading to underestimates of the true ENSO diversity (Giese et al. 2010).

Proxies for tropical Pacific climate, including corals, tree rings, lake sediments, and ice cores from alpine glaciers, provide a longer-term view of equatorial Pacific climate and ENSO variability before the instrumental era (Emile-Geay et al. 2013a,b; McGregor et al. 2013). For example, a 7,000-yr record from central Pacific corals (Cobb et al. 2013) suggests a strong decadal-to-centennial modulation of ENSO, in qualitative agreement with the amplitude modulation seen in unforced coupled general circulation model (CGCM) simulations (Wittenberg 2009; Stevenson et al. 2012; Deser et al. 2012; Wittenberg et al. 2014). However, relative to proxy reconstructions, unforced CGCMs tend to underestimate tropical multidecadal variability and may be too sensitive to external forcing (Ault et al. 2013). In these central Pacific coral records, the inferred interannual variance over the past 1,000 years is statistically indistinguishable from that during the mid-Holocene (6,000 years ago, or 6ka), in contrast to proxy records from the east Pacific (Moy et al. 2002; Conroy et al. 2008), which suggest reduced interannual variability at 6ka, as do mid-Holocene model simulations (Zheng et al. 2008; An and Choi 2013). One interpretation of these proxy results is that ENSO SST variability was displaced westward at 6ka. Indeed, results from a modeling study suggest larger SSTA differences in the eastern Pacific between the early and mid-Holocene (Braconnot et al. 2012), an indication of potentially greater uncertainty in that region. Thus, paleoclimate research offers a broader view of ENSO diversity, although the sparseness of proxy records and the remaining uncertainties in their interpretation do not yet allow a detailed description of that diversity.

Ocean reanalyses (e.g., Carton and Giese 2008; Zhang et al. 2007; Sun et al. 2007) can provide an alternative approach to reconstructed datasets, as they do not constrain historical SSTAs to look like the SSTA patterns associated with ENSO in recent years, and use both atmospheric information (surface heat and momentum fluxes) and ocean information (surface and subsurface observations, plus oceanic dynamics simulated by an ocean GCM). For example, a recent version of the Simple Ocean Data Assimilation (SODA; Carton and Giese 2008) has been forced with atmospheric fields [the twentieth-century reanalysis; Compo et al. (2011)] spanning the period 1871–2008, providing a relatively long record for ENSO diversity studies (Giese and Ray 2011)—albeit still subject to secular changes in the observing system [e.g., for the surface fluxes; Wittenberg (2004)]. Giese and Ray (2011) used the first moment of the equatorial SSTAs [center of heat index (CHI)] to examine the joint distribution of the longitude and strength of ENSO events in the 138-yr SODA reanalysis. Their analysis focuses on events with near-equatorial SSTAs exceeding 0.5°C in magnitude over an area as large (or larger) than the Niño-3.4 region (5°S–5°N, 120°–170°W). Their results indicate that the CHIs span a broad range of longitudes centered around 140°W, with a distribution that is statistically indistinguishable from Gaussian. The characterization of ENSO diversity based on SST statistics and SST-based indices focuses on the oceanic signature of El Niño and does not necessarily account for the coupled ocean–atmosphere signature of ENSO. Other studies (e.g., Chiodi and Harrison 2013) have considered parameters that are more characteristic of ocean–atmosphere coupling, such as the eastern equatorial Pacific outgoing longwave radiation. An index combining coupled SSTA and precipitation anomalies may be a good indicator of the most extreme teleconnections of ENSO (Cai et al. 2014).

Climate models can provide long simulations that include complete surface and subsurface information, to examine ENSO diversity in greater detail. In particular, phases 3 and 5 of the Climate Model Intercomparison Project (CMIP3 and CMIP5, respectively) include long simulations performed with numerous models, thus allowing the examination of ENSO diversity across a large multimodel ensemble. However, climate models have biases, for example, El Niño SSTA patterns that peak too far west. These biases, found in both the CMIP3 (Capotondi et al.

Unauthenticated | Downloaded 12/18/20 10:22 AM UTC

2006; Capotondi 2010; Guilyardi et al. 2009) and CMIP5 (Bellenger et al. 2014; Yang and Giese 2013) simulations, are extreme in some models and may limit their ability to reproduce the observed range of ENSO flavors (Ham and Kug 2012). A few models, however, can reproduce ENSO diversity with some realism (Yu and Kim 2010; Kim and Yu 2012) and can provide valuable insights.

For example, a 4,000-yr preindustrial control simulation from the Geophysical Fluid Dynamics Laboratory Climate Model, version 2.1 (GFDL CM2.1) captures much of the observed diversity of ENSO, although it significantly overestimates the amplitude of the ENSO interannual variability. This simulation has provided a detailed look at the distribution of the model's ENSO events (Delworth et al. 2006; Wittenberg et al. 2006, 2014; Wittenberg 2009; Kug et al. 2010). Because this simulation uses unchanging external forcings, its ENSO diversity is entirely intrinsically generated. The scatterplot in Fig. 3 shows the peak December–February (DJF) SSTA along the equator—and the corresponding longitude where that peak occurs—for every warm event in this simulation. The events with west Pacific SSTA peaks are weak, and those with central Pacific peaks are intermediate in strength, in agreement with the observationally based scatterplot in Fig. 1. Also similar to Fig. 1, the strongest events always peak in the east Pacific, although east Pacific events can exhibit a wide range of amplitudes. While the marginal distribution of CM2.1-simulated peak amplitudes (Fig. 3c) offers no evidence of bimodality, the marginal distribution of peak longitudes (Fig. 3a) does have a weakly bimodal character, with a tendency for SSTAs to peak most frequently near either 160°E (albeit farther west than observed) or 115°W. However, characterizing the simulated warm events as consisting of purely "western" and "eastern" types would be at odds with the bivariate distribution (Fig. 3b), which actually shows a continuum of events whose peaks shift eastward as they strengthen, plus a smaller group of weak EP events.

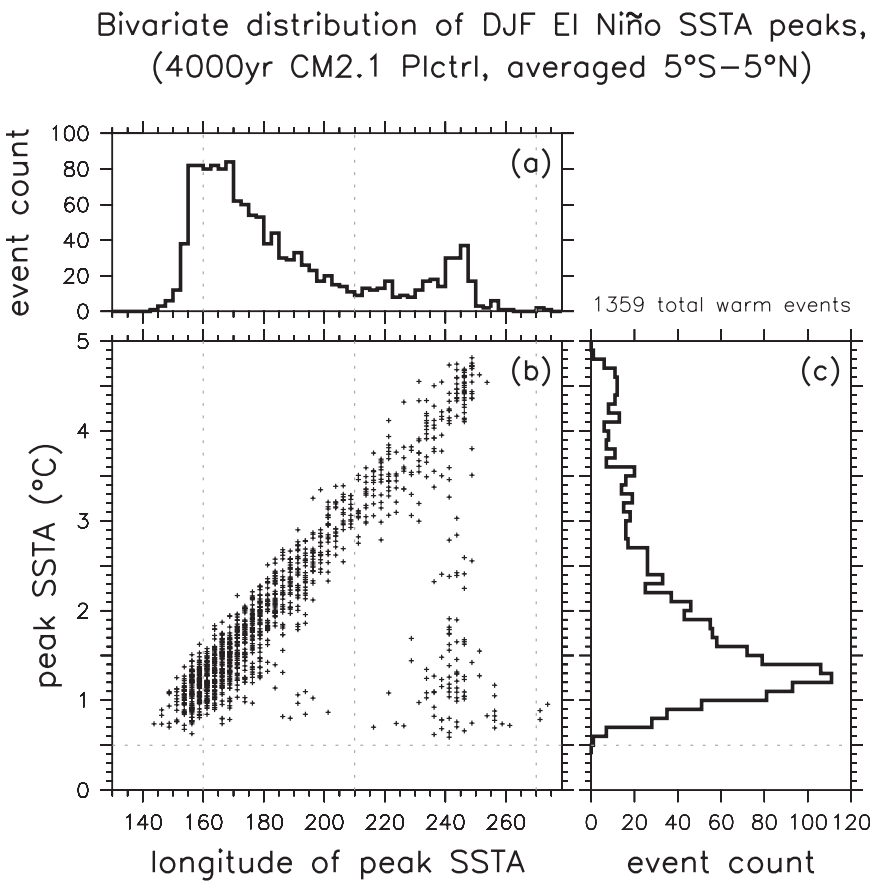

Fig. 3. Distribution of equatorial Pacific SSTA maxima, for El Niño events occurring in a 4,000-yr preindustrial control simulation from the GFDL CM2.1–coupled GCM. To qualify as an El Niño, the simulated DJF-mean SSTA averaged over the Niño-3 region (5°S–5°N, 150°–90°W) must exceed 0.5°C. For each of the 1,359 such events, the DJF-mean SSTA is averaged over the equatorial zone (5°S–5°N), and then the Pacific zonal maximum is located. (a) Distribution of peak SSTA longitudes (°E). (b) Scatterplot of the peak SSTA value (°C) vs the longitude (°E) at which it occurs. (c) Distribution of peak SSTA values (°C).

Millennia-long simulations from the GFDL CM2.1 and the National Center for Atmospheric Research (NCAR) Community Climate System Model, version 4 (CCSM4) have allowed a detailed analysis of the leading dynamical processes of events peaking at different longitudes, with results that are consistent with the view of ENSO diversity that has emerged from the shorter observational record. The quasi-cyclic ENSO evolution involves the movement of the upper-ocean warm water volume (WWV) to and from the equatorial thermocline, a process known as WWV

Unauthenticated | Downloaded 12/18/20 10:22 AM UTC

recharge–discharge (Jin 1997; Meinen and McPhaden 2000). The equatorial thermocline, the layer of large vertical density gradients that separates the warmer and active upper ocean from the colder deep ocean, is shallower in the eastern Pacific and deepens westward. Changes in the depth of the thermocline associated with the recharge–discharge processes are more influential on SST in the eastern Pacific, where the thermocline is shallower than in the western Pacific. Horizontal advection, especially the advection of the large zonal temperature gradients by the anomalous zonal currents, known as the zonal advective feedback, is another key process in the development of SST anomalies associated with ENSO. The zonal advective feedback tends to be more effective in the central Pacific, due to the large mean zonal SST gradients near the edge of the western Pacific Warm Pool. Thus, the leading dynamical processes differ with event location, with thermocline anomalies and recharge–discharge processes becoming progressively weaker as events peak farther west (Kug et al. 2010; Capotondi 2013).

Figure 4, for example, shows that for simulated events peaking in the Niño-3 region (Fig. 4a) the equatorial thermocline depth anomalies achieve their maximum depth (recharged state) a few months before the peak of the event (1 January) and then decrease rapidly afterward, an indication of the discharge of the warm water volume from the equatorial thermocline to higher latitudes. For events peaking in the Niño-4 region (Fig. 4b), the equatorial thermocline undergoes a similar evolution, but much weaker, while for events peaking in the westernmost region (Fig. 4c) the thermocline anomalies are very weak and remain of the same sign throughout the event evolution, indicating the absence of warm water discharge.

Zonal advection and air–sea heat fluxes, on the other hand, are relatively more important in the heat budget of the central Pacific SST anomalies, as has also been found in observational studies (Kao and Yu 2009; Kug et al. 2009, 2010; Yu et al. 2010; Lübbecke and McPhaden 2014; Newman et al. 2011a). In particular, using a variety of reanalysis products, Lübbecke and McPhaden (2014) find a weakening of the thermocline feedback, relative to the zonal advective feedback, in the eastern equatorial Pacific during the CP-dominated 2000–10 decade.

TELECONNECTIONS AND IMPACTS. SSTAs associated with the ENSO cycle influence convective processes and modify the atmospheric circulation, thus affecting patterns of weather variability worldwide (Trenberth et al. 1998). These atmospheric

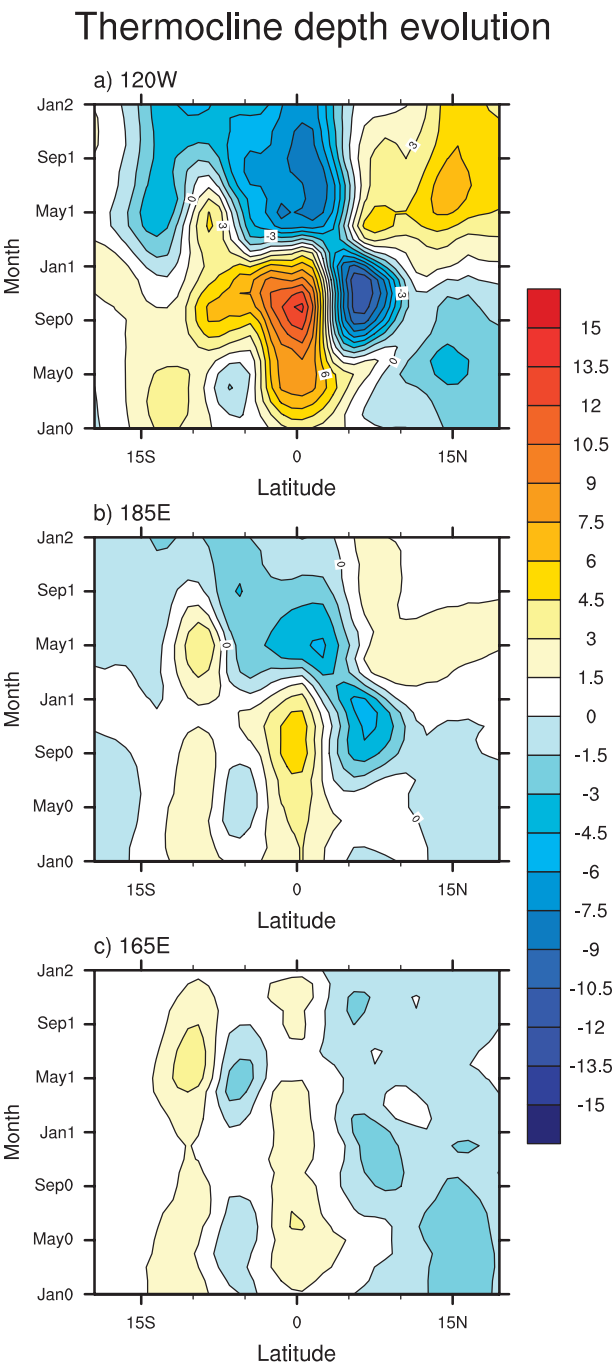

Fig. 4. Composite evolution of zonally averaged thermocline depth, displayed as a function of latitude and time, for El Niño events occurring in a 500-yr preindustrial control simulation from the NCAR CCSM4–coupled GCM. The selected events peak in (a) the Niño-3 region (5°S–5°N, 150°–90°W), (b) the Niño-4 region (5°S–5°N, 160°E–150°W), and (c) a region displaced 20° to the west of the Niño-4 area. The label at the top of each panel indicates the central longitude of the region where each event peaks. The date 1 Jan corresponds to the event peak, and the evolution is shown from Jan of year 0 to the Jan of year 2. The depth of the 15°C isotherm (m) is used as a proxy for thermocline depth. [Adapted from Capotondi (2013).]

Unauthenticated | Downloaded 12/18/20 10:22 AM UTC

teleconnections can be strongly influenced by key details of the equatorial SSTA pattern. The atmosphere tends to be most responsive to SSTAs in the Indo-Pacific warm pool region, where the surface is warm and atmospheric deep convection is most active, and less sensitive to SSTAs in the eastern Pacific cold tongue. However, SSTAs are stronger in the eastern Pacific, and the combination of atmospheric sensitivity and SSTA amplitude leads to the central equatorial Pacific playing a key role in remote impacts (Barsugli and Sardeshmukh 2002; Shin et al. 2010).

Through atmospheric teleconnections, ENSO influences the evolution of extratropical modes of atmospheric variability. The strength of the Aleutian low, the leading mode of North Pacific sea level pressure (SLP) variability, is influenced by SSTAs in both the eastern and central equatorial Pacific (Yu and Kim 2011). SSTAs in the central Pacific, however, have greater impact upon the second mode of North Pacific SLP variability, the North Pacific Oscillation (NPO) at decadal time scales (Di Lorenzo et al. 2010). The NPO is the atmospheric driver of the North Pacific Gyre Oscillation (NPGO), a mode of sea surface height (SSH) and SST variability that is connected with fluctuations of physical quantities (e.g., salinity, nutrients, chlorophyll-A) that are crucial for planktonic ecosystem dynamics in the northeast Pacific (Di Lorenzo et al. 2008).

The influences of tropical Pacific SSTAs associated with ENSO on precipitation and surface air temperatures over many parts of the globe have been outlined in the seminal papers of Ropelewski and Halpert (1987) and Halpert and Ropelewski (1992). Robust features include warm wintertime temperatures over the northern United States and western Canada and excess precipitation over the southeastern United States. However, CP events in recent years appear to be associated with different temperature and precipitation impacts over the United States (Larkin and Harrison 2005, hereafter LH05; Figs. 5 and 6). For example, during the fall season, EP events (defined as "conventional" by LH05) are associated with cooling in the central United States, while during CP events ("dateline" events in LH05's definition) the central United States experiences warming. In winter, the large warming in the northwestern United States during EP events is absent during CP events. Instead, cooling in the southeastern United States is observed (Fig. 5). Similarly, the pattern and even sign of precipitation anomalies over the United States differ for the two event types (Fig. 6). However, the patterns shown in Figs. 5 and 6 are based on a relatively small number of cases, so that large uncertainties remain on the temperature and precipitation anomaly patterns associated with the EP and CP events, as well as their differences.

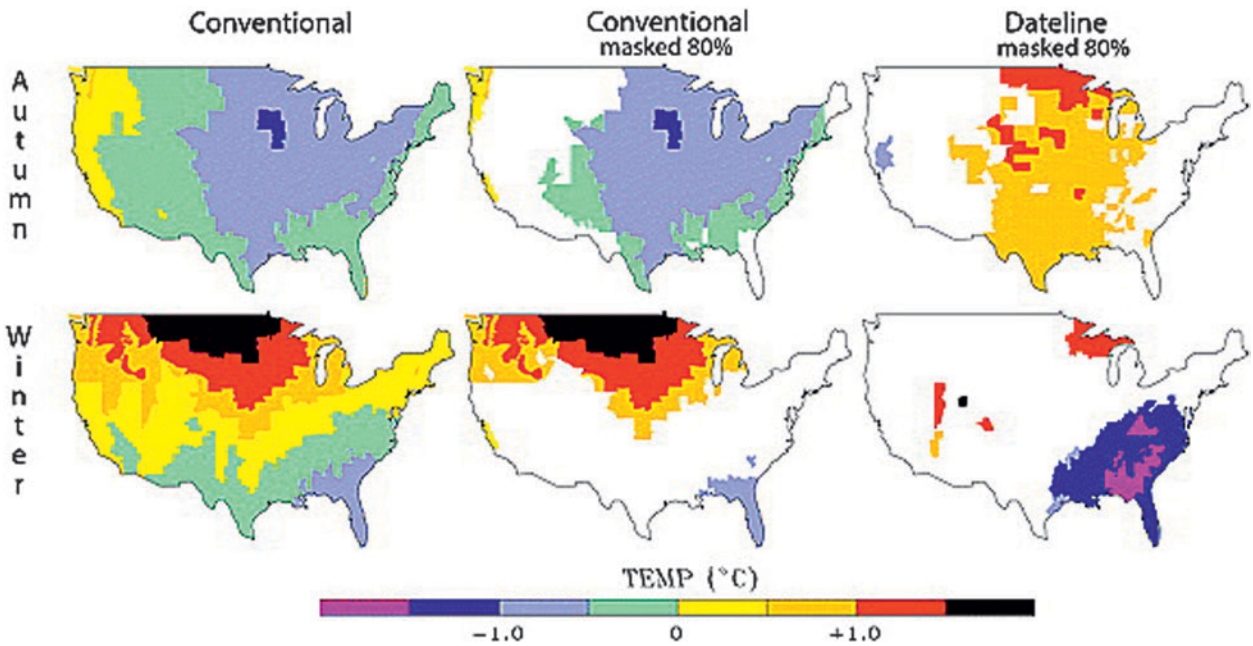

Fig. 5. Composites of U.S. temperature anomalies during autumn [Sep–Nov (SON)] and winter (DJF) for conventional (i.e., EP) and dateline (i.e., CP) El Niños during 1950–2003. Anomalies are computed relative to the 1950–95 climatology. The right two columns are masked for 80% statistical significance. (From LH05; courtesy of Drs. N. K. Larkin and D. E. Harrison.)

Unauthenticated | Downloaded 12/18/20 10:22 AM UTC

El Niño events have also been associated with reduced precipitation over northern, central, and peninsular India (Rasmusson and Carpenter 1982; Shukla and Paolino 1983; Ropelewski and Halpert 1987), as well as over northern and eastern Australia (Wang and Hendon 2007; Cai and Cowan 2009; Taschetto and England 2009). The location of SSTAs along the equatorial Pacific appears to be a very important factor for the reduced precipitation over both India and Australia, with events peaking in the central Pacific being much more influential than strong events peaking in the eastern Pacific. Thus, moderate El Niño events, like the 2002 and 2004 CP events, have resulted in severe and economically devastating droughts in both India (Kumar et al. 2006) and Australia (Wang and Hendon 2007), while the very strong 1997/98 El Niño had very little effect on precipitation in both regions. It should be noted, however, that due to the brevity of the observational record, the relationship between El Niño events and summertime Indian rainfall remains overall uncertain for both EP and CP event types. La Niña events are associated with increased precipitation over Australia, with marked differences between EP and CP types (Cai and Cowan 2009).

The large influence of CP El Niños on Southern Hemisphere wintertime storm-track activity (Ashok et al. 2007) appears to have important implications for the temperature anomalies over Antarctica (T. Lee et al. 2010). The locations of SSTAs may also have an impact on the frequency and trajectory of North Atlantic tropical cyclones. Cyclone activity is usually reduced during El Niño and enhanced during La Niña. However, warming in the central Pacific has been associated with an increased frequency of North Atlantic tropical cyclones, with enhanced likelihood of landfall along the Gulf of Mexico and Central America (Kim et al. 2009). Some of the El Niño years considered by Kim et al. (2009) were also characterized by a broader Atlantic warm pool (AWP) extent (S.-K. Lee et al. 2010), making it unclear which of these two factors (central equatorial Pacific warming or AWP size) has been the primary cause of tropical Atlantic cyclone activity.

Apart from extratropical influences, the different spatial patterns of SSTAs during EP and CP events have considerable socioeconomic consequences in the tropics (McPhaden 2004). During large EP El Niño events, warming in the eastern Pacific leads to a southward shift of the intertropical convergence zone, resulting in intense rainfall over eastern Pacific regions that are normally dry, with greater incidences of catastrophic floods in parts of Ecuador and northern Peru. In contrast during CP events, cooler conditions can exist in the eastern Pacific (Dewitte et al. 2012), producing dryness in Peru and Ecuador during the usual rainy season, with disruptions to local agriculture.

The ocean circulation changes associated with different ENSO types have distinct impacts on

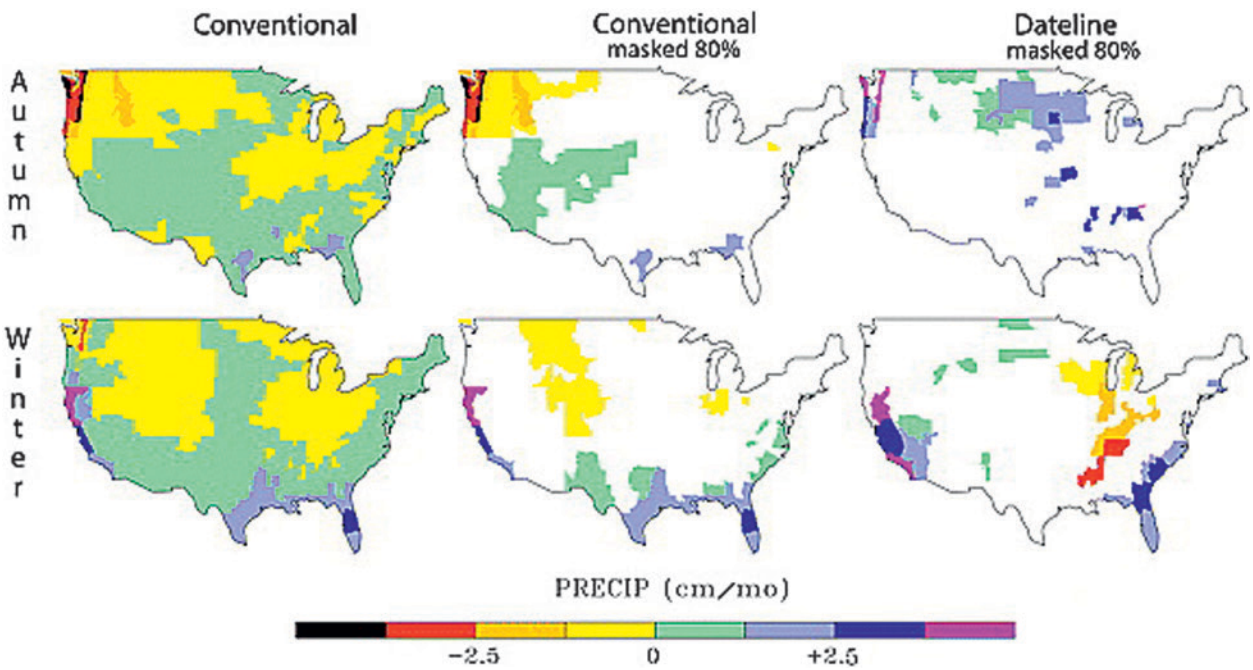

Fig. 6. As in Fig. 5, but for U.S. precipitation anomalies.

Unauthenticated | Downloaded 12/18/20 10:22 AM UTC

biological processes along the equator. Classical EP El Niños are known to reduce eastern Pacific chlorophyll-A concentrations, by deepening the ocean thermocline and weakening the upwelling of nutrient-rich deep waters in that region. The CP El Niños cause similar biological changes in the central Pacific rather than in the eastern Pacific (Turk et al. 2011; Radenac et al. 2012), but for different reasons, namely, stronger horizontal advection of nutrient-depleted warm pool waters toward the central equatorial Pacific (Gierach et al. 2012; Lee et al. 2014). Along the western coast of South America, CP and EP El Niños have been shown to have significantly different impacts on the upwelling off Peru, with a tendency for colder SSTs during CP El Niño events (Dewitte et al. 2012). Decadal variations in the relative frequency of EP and CP events would be expected to produce a restructuring of the marine ecosystems, with important implications for fisheries.

PREDICTABILITY AND PREDICTION. The predictability of ENSO events in general, and specific types in particular, relies on the existence of precursors or "triggers" (atmospheric and/or oceanic) responsible for the excitation of events at some lead time. Precursors within the equatorial Pacific are in the form of intraseasonal atmospheric disturbances known as westerly wind events (WWEs) or westerly wind bursts (WWBs; McPhaden 1999; McPhaden and Yu 1999; Fedorov 2002). WWEs occur over a broad range of longitudes in the central western Pacific, and can excite eastward-propagating Kelvin waves that, in turn, favor the development of El Niño by deepening the eastern equatorial Pacific thermocline, creating positive SSTAs in the eastern Pacific, and leading to a weakening of the trade winds and to a further deepening of the thermocline, a positive feedback cycle known as the Bjerknes feedback. The timing, strength, and longitudinal location of the WWEs appear to be very important in the development of either EP or CP events (Karnauskas 2013; Harrison and Chiodi 2009). While the efficiency of WWEs in triggering El Niño events has been documented from observations (McPhaden and Yu 1999), the short duration of the instrumental record does not allow a full understanding of the mechanistic link between ENSO and WWEs.

Recent numerical experiments have also highlighted the importance of the ocean background conditions in determining the type of El Niño resulting from WWE activity. If the tropical Pacific upper-ocean heat content is larger than normal, a condition referred to as a recharged state, WWEs can lead to an EP El Niño (Lengaigne et al. 2004), while for the upper ocean heat content levels that are near average ("neutral") WWEs may result in a CP El Niño (Fedorov et al. 2015). WWE prevalence, in turn, depends on the zonal extent of the west Pacific warm pool, which is a function of both the background climatological state and ENSO (Eisenman et al. 2005; Vecchi et al. 2006). This could result in a coupled, nonlinear interplay among the WWEs, ENSO, and the decadal background state (Gebbie et al. 2007; Zavala-Garay et al. 2008; Sun and Yu 2009; Harrison and Chiodi 2009; Ogata et al. 2013; Choi et al. 2013).

Off-equatorial atmospheric variability can also play an important role in triggering ENSO events. In particular, the NPO is associated with wind anomalies that impart a "footprint" on the ocean through changes in surface heat fluxes. The SST footprint, which is termed the North Pacific meridional mode (NPMM) because of its association with a subtropical north–south SST gradient that peaks in spring and persists through summer (Chiang and Vimont 2004; Chang et al. 2007), has been shown to trigger ENSO events (Larson and Kirtman 2013). This mode exerts a positive feedback that further weakens the winds and strengthens the existing SSTAs. This positive SST feedback, known as the wind–evaporation–SST (WES) feedback (Xie 1999), supports a southwestward coevolution of the oceanic SSTAs and wind anomalies that ultimately reaches the tropics, favoring the development of an El Niño event through the excitation of downwelling equatorial Kelvin waves.

Apart from this thermodynamic coupling, the NPO-related wind anomalies can dynamically energize equatorial processes through the excitation of off-equatorial Rossby waves (Alexander et al. 2010), as well as changes in the strength of the tropical upper-ocean overturning circulation (Anderson et al. 2013). This NPO-related forcing has been associated with CP events (Yu and Kim 2011, Kim et al. 2012; Vimont et al. 2014). As for the WWEs, the selection of the type of ENSO response may depend upon the mean state of the equatorial ocean, whether recharged, neutral, or discharged (Anderson 2007; Alexander et al. 2010; Deser et al. 2012).

An SSTA pattern similar to the NPMM exists also in the Southern Hemisphere, and has been termed the South Pacific meridional mode (SPMM) by Zhang et al. (2014). Although similar in nature to the NPMM, the SPMM extends all the way to the eastern and central equatorial Pacific, while the NPMM is limited to the Northern Hemisphere subtropics. It is possible that the SPMM is more effective in exciting eastern Pacific events, while the NPMM may be more effective in triggering central Pacific events (Zhang et al. 2014; Vimont et al. 2014).

Unauthenticated | Downloaded 12/18/20 10:22 AM UTC

As the existence of possible precursors indicates some seasonal-to-interannual predictability of the various ENSO flavors, the ability of state-of-the-art prediction systems to capture ENSO diversity has been examined in the North American Multimodel Ensemble (NMME) prediction experiment (Kirtman et al. 2014). The NMME system includes ensemble retrospective forecasts (1982–present) from nine different models. For lead times up to 6 months and from a qualitative basin-scale perspective, the models are able to capture some of the observed contrasts between the warming in the east versus west Pacific and the associated differences in the rainfall anomalies. However, the models systematically produce too much warming in the east compared to the observational estimates for events centered in the central/western Pacific, so that the strong eastern Pacific events are demonstrably better predicted at both short and long lead times.

ENSO prediction skill at more than a 3-month lead time largely originates from the oceanic memory associated with the equatorial Pacific upper-ocean heat content. The WWV index, defined as the average depth of the 20°C isotherm in the equatorial band, has been shown to be a good predictor of ENSO events two to three seasons in advance (Meinen and McPhaden 2000). The changes in the recharge–discharge processes associated with the higher frequency of CP events since 2000 have reduced the role of the WWV index as a predictor (Hendon et al. 2009, McPhaden 2012), and degraded the predictive skills of seasonal forecast models for the 2002–11 period relative to the 1980s and 1990s (Wang et al. 2010; Barnston et al. 2012; Xue et al. 2013).

On longer time scales, paleoclimate records and climate simulations exhibit epochs of extreme ENSO behavior that can persist for decades (e.g., Wittenberg 2009; Stevenson et al. 2012; McGregor et al. 2013; Cobb et al. 2013; Karamperidou et al. 2014). Model simulations suggest that epochs with an abundance of strong, EP-type El Niños tend to be associated with decadally warm conditions in the east Pacific, and decadally cooler conditions in the west (Choi et al. 2011, 2012), which may in large part be due to the rectification of the ENSO signal (Rodgers et al. 2004; Schopf and Burgman 2006; Ogata et al. 2013). The extent to which decadal variations (either intrinsic to the climate system or ENSO driven) affect ENSO behavior is not yet clear. Experiments with the GFDL CM2.1 control simulation (Wittenberg et al. 2014), in which the model's own multidecadal epochs of extreme ENSO behavior were reforecast using a "perfect model" setup with only tiny perturbations to the initial conditions, indicated no inherent decadal-scale predictability of ENSO behavior (amplitude, frequency, or type), suggesting that in the absence of changes in external forcings, such multidecadal extreme epochs could occur at random.

ENSO DIVERSITY AND CLIMATE CHANGE. The abundance of events with SSTAs peaking in the central Pacific over the last 20 years (Lee and McPhaden 2010), as compared to prior decades, has been suggested as a possible harbinger of changes in ENSO characteristics due to global warming (Yeh et al. 2009). Indeed, the ratio of CP- to EP-type events (at least in terms of SST patterns) is projected to increase in the CMIP3 climate model simulations under global warming scenarios (Yeh et al. 2009), with similar results for the CMIP5 simulations (Kim and Yu 2012). Climate models project a weakening of the climatological Walker circulation as a result of global warming (Vecchi et al. 2006; Xie et al. 2010), with a consequent weakening of the zonal slope of the equatorial thermocline, and a weaker eastern equatorial Pacific cold tongue. These changes have been suggested as possible drivers of the recent increase in the occurrence of CP-type events. While the weakened trade winds and weakened equatorial upwelling reduce ENSO SSTAs in the eastern Pacific (by reducing the thermocline feedback), the increased thermal stratification of the sloping thermocline enhances ENSO SSTAs in the central Pacific, by strengthening both subsurface zonal advective feedbacks (DiNezio et al. 2012) and thermocline feedbacks (Dewitte et al. 2013) in that region. Interestingly, extreme El Niño events in terms of equatorial *rainfall* patterns, resembling the 1982/83 and 1997/98 cases, are also projected to increase in frequency due to global warming (Cai et al. 2014).

While climate models project a weaker Walker circulation pattern, results from observations and atmospheric reanalyses provide contrasting results on whether equatorial surface winds have indeed weakened, stayed the same, or even strengthened in recent decades (e.g., Tokinaga et al. 2012a; Solomon and Newman 2012; L'Heureax et al. 2013; Sandeep et al. 2014), making ENSO projections in a changing climate highly uncertain.

So far, the impact of climate change on ENSO diversity has been difficult to evaluate, given that ENSO behavior may be intrinsically modulated even in the absence of external forcing (Zebiak and Cane 1987; Wittenberg 2009). The random combinations of initial optimal structures obtained with a linear stochastic model (Newman et al. 2011b; Fig. 2, top) can produce extended epochs dominated by either

Unauthenticated | Downloaded 12/18/20 10:22 AM UTC

type of event, without the need for anthropogenic changes in the background state. This behavior is also seen in coupled GCMs, where unforced control runs can spontaneously generate multidecade epochs populated entirely by CP or EP events (Kug et al. 2010; Choi et al. 2011; Wittenberg et al. 2014).

This intrinsic modulation of ENSO can in turn affect the multidecadal background state, confounding detection of anthropogenic influences in short climate records. In unforced climate simulations, epochs with greater incidence of the weaker, CP-like El Niños appear to steepen the equatorial time-mean thermocline slope and zonal SST gradient (Rodgers et al. 2004; Ogata et al. 2013). Indeed, an analysis of SST observations over the past three decades (Lee and McPhaden 2010) suggests that the increasing amplitude of El Niño in the central Pacific contributed to the well-observed multidecadal warming in this region, thus enhancing the zonal SST gradient. In addition, McPhaden et al. (2011) showed from observations that the equatorial thermocline steepened in moving from 1980–99 (when EP events prevailed) to 2000–10 (when CP events prevailed). This would seem to contrast with the anthropogenic response described above, in which a weakened time-mean zonal SST gradient, and a flatter but more intense thermocline, favor CP events. However, given the substantial remaining uncertainty regarding the magnitude (and even the sign) of the anthropogenic impacts and of ENSO's interactions with the mean state (Vecchi and Wittenberg 2010; Collins et al. 2010; Compo and Sardeshmukh 2010; DiNezio et al. 2010, 2012; Solomon and Newman 2012; Tokinaga et al. 2012a,b), it is not yet clear to what extent observed ENSO modulation is a cause or a consequence of either anthropogenic or intrinsic decadal-scale changes in the equatorial Pacific mean state.

CONCLUSIONS. The last decade has seen exciting advances in ENSO research. Differences among ENSO events, although recognized for a long time, have been examined in greater depth, and it has become increasingly clear that the details of the spatial patterns associated with ENSO affect its atmospheric teleconnections and impacts. Examinations of observations, climate reanalyses, and climate models show that while the essential physical processes underlying the different ENSO types are the same, their relative roles may vary in driving SSTAs at different longitudes. For example, the thermocline feedback is more effective at driving SSTAs in the eastern Pacific, where the thermocline is closer to the surface, while zonal advection near the edge of the warm pool is most effective at driving SSTAs in the central Pacific. Strong events, which usually peak in the eastern Pacific, may also involve nonlinear processes. Thus, ENSO can be described as a coupled atmosphere–ocean phenomenon that exhibits substantial variations with regionally different feedbacks, leading to a diverse continuum of realized ENSO events.

As our understanding of ENSO broadens, new questions arise:

1) How is ENSO diversity influenced by decadal-to-centennial-scale changes in radiative forcings and the climatological background state?
2) What are the sources and limits of predictability, both tropical and extratropical, associated with the differences in ENSO events?
3) How can climate models be improved to more properly simulate ENSO diversity?
4) Can we improve forecasts of ENSO flavors in operational ENSO prediction systems?

To answer these questions, further studies are needed using observational and reanalysis datasets, paleoclimate records, and model simulations. Sustained and enhanced climate observations, better models, and improved understanding are all imperative for more reliable ENSO monitoring and prediction in a changing climate.

ACKNOWLEDGMENTS. The authors of this paper are members of the U.S. CLIVAR ENSO Diversity Working Group, sponsored by U.S. CLIVAR. The working group wishes to acknowledge the U.S. CLIVAR office for its support, and the U.S. CLIVAR funding agencies, NASA, NOAA, NSF, and DOE, for their sponsorship. The authors would also like to thank Drs. M. McPhaden and D. Dommenget, as well as two anonymous reviewers, for their careful readings of the manuscript, excellent suggestions, and constructive criticism, which have considerably improved the paper. Part of this research was carried out at the Jet Propulsion Laboratory, California Institute of Technology, under a contract with the National Aeronautics and Space Administration. AC acknowledges support from the National Science Foundation for this study.

REFERENCES

Alexander, M. A., D. J. Vimont, P. Chang, and J. D. Scott, 2010: The impact of extratropical atmospheric variability on ENSO: Testing the seasonal footprinting mechanism using coupled model experiments. *J. Climate,* **23,** 2885–2901, doi:10.1175/2010JCLI3205.1.

Unauthenticated | Downloaded 12/18/20 10:22 AM UTC

An, S.-I., and J. Choi, 2013: Mid-Holocene tropical Pacific climate state, annual cycle, and ENSO in PMIP2 and PMIP3. *Climate Dyn.,* **43,** 957–970, doi:10.1007/s00382-013-1880-z.

Anderson, B. T., 2007: On the joint role of subtropical atmospheric variability and equatorial subsurface heat content anomalies in initiating the onset of ENSO events. *J. Climate,* **20,** 1593–1599, doi:10.1175/JCLI4075.1.

——, R. Perez, and A. Karspeck, 2013: Triggering of El Niño onset through the trade-wind induced charging of the equatorial Pacific. *Geophys. Res. Lett.,* **40,** 1212–1216, doi:10.1002/grl.50200.

Ashok, K., S. K. Behera, S. A. Rao, H. Weng, and T. Yamagata, 2007: El Niño Modoki and its possible teleconnections. *J. Geophys. Res.,* **112,** C11007, doi:10.1029/2006JC003798.

Ault, T., C. Deser, M. Newman, and J. Emile-Geay, 2013: Characterizing decadal to centennial variability in the equatorial Pacific during the last millennium. *Geophys. Res. Lett.,* **40,** 3450–3456, doi:10.1002/grl.50647.

Barnston, A. G., M. K. Tippett, M. L. L'Heureux, S. Li, and D. G. DeWitt, 2012: Skill of real-time seasonal ENSO model predictions during 2002–11: Is our capability increasing? *Bull. Amer. Meteor. Soc.,* **93,** 631–651, doi:10.1175/BAMS-D-11-00111.1.

Barsugli, J. J., and P. Sardeshmukh, 2002: Global atmospheric sensitivity to tropical SST anomalies throughout the Indo-Pacific basin. *J. Climate,* **15,** 3427–3442, doi:10.1175/1520-0442(2002)015<3427:GASTTS>2.0.CO;2.

Bellenger, H., E. Guilyardi, J. Leloup, M. Lengaigne, and J. Vialard, 2014: ENSO representation in climate models: From CMIP3 to CMIP5. *Climate Dyn.,* **42,** 1999–2018, doi:10.1007/s00382-013-1783-z.

Braconnot, P., Y. Luan, S. Brewer, and W. Zheng, 2012: Impact of Earth's orbit and freshwater fluxes on Holocene climate mean seasonal cycle and ENSO characteristics. *Climate Dyn.,* **38,** 1081–1092, doi:10.1007/s00382-011-1029-x.

Cai, W., and T. Cowan, 2009: La Niña Modoki impacts Australia autumn rainfall variability. *Geophys. Res. Lett.,* **36,** L12805, doi:10.1029/2009GL037885.

——, and Coauthors, 2014: Increasing frequency of extreme El Niño events due to greenhouse warming. *Nat. Climate Change,* **4,** 111–116, doi:10.1038/nclimate2100.

Capotondi, A., 2010: ENSO ocean dynamics: Simulation by coupled general circulation models. *Climate Dynamics: Why Does Climate Vary?, Geophys. Monogr.,* Vol. 189, Amer. Geophys. Union, 53–64.

——, 2013: ENSO diversity in the NCAR CCSM4 climate model. *J. Geophys. Res. Oceans,* **118,** 4755–4770, doi:10.1002/jgrc.20335.

——, A. T. Wittenberg, and S. Masina, 2006: Spatial and temporal structure of tropical Pacific interannual variability in 20th century climate simulations. *Ocean Modell.,* **15,** 274–298, doi:10.1016/j.ocemod.2006.02.004.

Carton, J. A., and B. S. Giese, 2008: A reanalysis of ocean climate using Simple Ocean Data Assimilation (SODA). *Mon. Wea. Rev.,* **136,** 2999–3017, doi:10.1175/2007MWR1978.1.

Chang, P., L. Zhang, R. Saravanan, D. J. Vimont, J. C. H. Chiang, L. Ji, H. Seidel, and M. K. Tippett, 2007: Pacific meridional mode and El Niño–Southern Oscillation. *Geophys. Res. Lett.,* **34,** L16608, doi:10.1029/2007GL030302.

Chiang, J. C. H., and D. J. Vimont, 2004: Analogous Pacific and Atlantic meridional modes of tropical atmosphere–ocean variability. *J. Climate,* **17,** 4143–4158, doi:10.1175/JCLI4953.1.

Chiodi, A. M., and D. E. Harrison, 2013: El Niño impacts on seasonal U.S. atmospheric circulation, temperature, and precipitation anomalies: The OLR-event perspective. *J. Climate,* **26,** 822–837, doi:10.1175/JCLI-D-12-00097.1.

Choi, J., S.-I. An, J.-S. Kug, and S.-W. Yeh, 2011: The role of mean state on changes in El Niño flavor. *Climate Dyn.,* **37,** 1205–1215, doi:10.1007/s00382-010-0912-1.

——, ——, and S.-W. Yeh, 2012: Decadal amplitude modulation of two types of ENSO and its relationship with the mean state. *Climate Dyn.,* **28,** 2631–2644, doi:10.1007/s00382-011-1186-y.

Choi, K.-Y., G. A. Vecchi, and A. T. Wittenberg, 2013: ENSO transition, duration, and amplitude asymmetries: Role of the nonlinear wind stress coupling in a conceptual model. *J. Climate,* **26,** 9462–9476, doi:10.1175/JCLI-D-13-00045.1.

Cobb, K. M., N. Westphal, H. Sayani, E. Di Lorenzo, H. Cheng, R. L. Edwards, and C. D. Charles, 2013: Highly variable El Niño–Southern Oscillation throughout the Holocene. *Science,* **339,** 67–70, doi:10.1126/science.1228246.

Collins, M., and Coauthors, 2010: The impact of global warming on the tropical Pacific and El Niño. *Nat. Geosci.,* **3,** 391–397, doi:10.1038/ngeo868.

Compo, G., and P. D. Sardeshmukh, 2010: Removing ENSO-related variations from the climate record. *J. Climate,* **23,** 1957–1978, doi:10.1175/2009JCLI2735.1.

Compo, G., and co-authors, 2011: The Twentieth Century Reanalysis Project. *Quart. J. Roy. Meteor. Soc.,* **137,** 1–28.

Conroy, J. L., J. T. Overpeck, J. E. Cole, T. M. Shanahan, and M. Steinitz-Kannan, 2008: Holocene changes in eastern tropical Pacific climate inferred from a

Unauthenticated | Downloaded 12/18/20 10:22 AM UTC

Galápagos lake sediment record. *Quat. Sci. Rev.,* **27,** 1166–1180, doi:10.1016/j.quascirev.2008.02.015.

Delworth, T. L., and Coauthors, 2006: GFDL's CM2 global coupled climate models. Part I: Formulation and simulation characteristics. *J. Climate,* **19,** 643–674, doi:10.1175/JCLI3629.1.

Deser, C., and Coauthors, 2012: ENSO and Pacific decadal variability in Community Climate System Model version 4. *J. Climate,* **25,** 2622–2651, doi:10.1175/JCLI-D-11-00301.1.

Dewitte, B., and Coauthors, 2012: Change in El Niño flavours over 1958–2008: Implications for the long-term trend of the upwelling off Peru. *Deep-Sea Res. II,* **77–80,** 143–156, doi:10.1016/j.dsr2.2012.04.011.

——, S.-W. Yeh, and S. Thual, 2013: Reinterpreting the thermocline feedback in the western-central equatorial Pacific and its relationship with the ENSO modulation. *Climate Dyn.,* **41,** 819–830, doi:10.1007/s00382-012-1504-z.

Di Lorenzo, E., and Coauthors, 2008: North Pacific Gyre Oscillation links ocean climate and ecosystem change. *Geophys. Res. Lett.,* **35,** L08607, doi:10.1029/2007GL032838.

——, K. M. Cobb, J. C. Furtado, N. Schneider, B. T. Anderson, A. Bracco, M. A. Alexander, and D. J. Vimont, 2010: Central Pacific El Niño and decadal climate change in the North Pacific Ocean. *Nat. Geosci.,* **3,** 762–765, doi:10.1038/ngeo984.

DiNezio, P. N., A. C. Clement, and G. A. Vecchi, 2010: Reconciling differing views of tropical Pacific climate change. *Eos, Trans. Amer. Geophys. Union,* **91,** 141–142, doi:10.1029/2010EO160001.

——, B. P. Kirtman, A. C. Clement, S.-K. Lee, G. A. Vecchi, and A. Wittenberg, 2012: Mean climate controls on the simulated response of ENSO to increasing greenhouse gases. *J. Climate,* **25,** 7399–7420, doi:10.1175/JCLI-D-11-00494.1.

Dommenget, D., T. Bayr, and C. Frauen, 2013: Analysis of the non-linearity in the pattern and time evolution of El Niño Southern Oscillation. *Climate Dyn.,* **40,** 2825–2847, doi:10.1007/s00382-012-1475-0.

Eisenman, I., L. Yu, and E. Tziperman, 2005: Westerly wind bursts: ENSO's tail rather than the dog? *J. Climate,* **18,** 5224–5238, doi:10.1175/JCLI3588.1.

Emile-Geay, J., K. Cobb, M. Mann, and A. T. Wittenberg, 2013a: Estimating central equatorial Pacific SST variability over the past millennium. Part I: Methodology and validation. *J. Climate,* **26,** 2302–2328, doi:10.1175/JCLI-D-11-00510.1.

——, ——, ——, and ——, 2013b: Estimating central equatorial Pacific SST variability over the past millennium. Part II: Reconstructions and implications. *J. Climate,* **26,** 2329–2352, doi:10.1175/JCLI-D-11-00511.1.

Fedorov, A. V., 2002: The response of the coupled tropical ocean–atmosphere to westerly wind bursts. *Quart. J. Roy. Meteor. Soc.,* **128,** 1–23, doi:10.1002/qj.200212857901.

——, S. Hu, M. Lengaigne, and E. Guilyardi, 2015: The impact of westerly wind bursts and ocean initial state on the development, and diversity of El Niño events. Climate Dyn., 44, 1381–1401, doi:10.1007/s00382-014-2126-4.

Gebbie, G., I. Eisenman, A. Wittenberg, and E. Tziperman, 2007: Modulation of westerly wind bursts by sea surface temperature: A semistochastic feedback for ENSO. *J. Atmos. Sci.,* **64,** 3281–3295, doi:10.1175/JAS4029.1.

Gierach, M. M., T. Lee, D. Turk, and M. J. McPhaden, 2012: Biological response to the 1997-98 and 2009-10 El Niño events in the equatorial Pacific Ocean. *Geophys. Res. Lett.,* **39,** L10602, doi:10.1029/2012GL051103.

Giese, B. S., and S. Ray, 2011: El Niño variability in simple ocean data assimilation (SODA), 1871–2008. *J. Geophys. Res.,* **116,** C02024, doi:10.1029/2010JC006695.

——, N. C. Slowey, S. Ray, G. P. Compo, P. D. Sardeshmukh, J. A. Carton, and J. S. Whitaker, 2010: The 1918/19 El Niño. *Bull. Amer. Meteor. Soc.,* **91,** 177–183, doi:10.1175/2009BAMS2903.1.

Graham, F. S., J. N. Brown, C. Langlais, S. J. Marsland, A. T. Wittenberg, and N. J. Holbrook, 2014: Effectiveness of the Bjerknes stability index in representing ocean dynamics. *Climate Dyn.,* **43,** 2399–2414, doi:10.1007/s00382-014-2062-3.

Guilyardi, E., A. Wittenberg, A. Fedorov, M. Collins, C. Wang, A. Capotondi, G. J. van Oldenborgh, and T. Stockdale, 2009: Understanding El Niño in ocean–atmosphere general circulation models: Progress and challenges. *Bull. Amer. Meteor. Soc.,* **90,** 325–340, doi:10.1175/2008BAMS2387.1.

Halpert, M. S., and C. F. Ropelewski, 1992: Surface temperature patterns associated with the Southern Oscillation. *J. Climate,* **5,** 577–593, doi:10.1175/1520-0442(1992)005<0577:STPAWT>2.0.CO;2.

Ham, Y.-G., and J.-S. Kug, 2012: How well do current climate models simulate two types of El Nino? *Climate Dyn.,* **39,** 383–398, doi:10.1007/s00382-011-1157-3.

Harrison, D. E., and A. M. Chiodi, 2009: Pre- and post-1997/98 westerly wind events and equatorial Pacific cold tongue warming. *J. Climate,* **22,** 568–581, doi:10.1175/2008JCLI2270.1.

Unauthenticated | Downloaded 12/18/20 10:22 AM UTC

Hendon, H. H., E. Lim, G. Wang, O. Alves, and D. Husdon, 2009: Prospects for predicting two flavors of El Niño. *Geophys. Res. Lett.,* **36,** L19713, doi:10.1029/2009GL040100.

Jin, F.-F., 1997: An equatorial ocean recharge paradigm for ENSO. Part I: Conceptual model. *J. Atmos. Sci.,* **54,** 811–829, doi:10.1175/1520-0469(1997)054<0811:AEORPF>2.0.CO;2.

——, S.-I. An, A. Timmermann, and J. Zhao, 2003: Strong El Niño events and nonlinear dynamical heating. *Geophys. Res. Lett.,* **30,** 1120, doi:10.1029/2002GL016356.

Kalnay, E., and Coauthors, 1996: NCEP/NCAR 40-Year Reanalysis Project. *Bull. Amer. Meteor. Soc.,* **77,** 437–471, doi:10.1175/1520-0477(1996)077<0437:TNYRP>2.0.CO;2.

Kao, H. Y., and J. Y. Yu, 2009: Contrasting eastern Pacific and central Pacific types of ENSO. *J. Climate,* **22,** 615–632, doi:10.1175/2008JCLI2309.1.

Karamperidou, C., M. A. Cane, U. Lall, and A. T. Wittenberg, 2014: Intrinsic modulation of ENSO predictability viewed through a local Lyapunov lens. *Climate Dyn.,* **42,** 253–270, doi:10.1007/s00382-013-1759-z.

Karnauskas, K. B., 2013: Can we distinguish canonical El Niño from Modoki? *Geophys. Res. Lett.,* **40,** 5246–5251, doi:10.1002/grl.51007.

Kim, H.-M., P. J. Webster, and J. A. Curry, 2009: Impact of shifting patterns of Pacific Ocean warming on North Atlantic tropical cyclones. *Science,* **325**, doi:10.1126/science.1174062.

Kim, J.-S., K.-Y. Kim, and S.-W. Yeh, 2012: Statistical evidence for the natural variation of the central Pacific El Nino. *J. Geophys. Res.,* **117,** C06014, doi:10.1029/2012JC008003.

Kim, S. T., and J.-Y. Yu, 2012: The two types of ENSO in CMIP5 models. *Geophys. Res. Lett.,* **39,** L11704, doi:10.1029/2012GL052006.

Kirtman, B. P., and Coauthors, 2014: The North American Multimodel Ensemble. *Bull. Amer. Meteor. Soc.,* **95,** 585–601, doi:10.1175/BAMS-D-12-00050.1.

Kug, J.-S., F.-F. Jin, and S.-I. An, 2009: Two types of El Niño events: Cold tongue El Niño and warm pool El Niño. *J. Climate,* **22,** 1499–1515, doi:10.1175/2008JCLI2624.1.

——, J. Choi, S.-I. An, F.-F. Jin, and A. T. Wittenberg, 2010: Warm pool and cold tongue El Niño events as simulated by the GFDL CM2.1 coupled GCM. *J. Climate,* **23,** 1226–1239, doi:10.1175/2009JCLI3293.1.

Kumar, K. K., B. Rajagopalan, M. Hoerling, G. Bates, and M. Cane, 2006: Unraveling the mystery of Indian monsoon failure during El Niño. *Science,* **314,** 115–118, doi:10.1126/science.1131152.

Larkin, N. K., and D. E. Harrison, 2005: On the definition of El Niño and associated seasonal average U.S. weather anomalies. *Geophys. Res. Lett.,* **32,** L13705, doi:10.1029/2005GL022738.

Larson, S., and B. P. Kirtman, 2013: The Pacific meridional mode as a trigger for ENSO in a high-resolution coupled model. *Geophys. Res. Lett.,* **40,** 3189–3194, doi:10.1002/grl.50571.

Lee, K.-W., S.-W. Yeh, J.-S. Kug, and J.-Y. Park, 2014: Ocean chlorophyll response to two types of El Nino events in an ocean-biogeochemical coupled model. *J. Geophys. Res. Oceans,* **119,** 933–952, doi:10.1002/2013JC009050.

Lee, S.-K., C. Wang, and D. B. Enfield, 2010: On the impact of central Pacific warming events on Atlantic tropical storm activity. *Geophys. Res. Lett.,* **37,** L17702, doi:10.1029/2010GL044459.

Lee, T., and M. J. McPhaden, 2010: Increasing intensity of El Niño in the central-equatorial Pacific. *Geophys. Res. Lett.,* **37,** L14603, doi:10.1029/2010GL044007.

——, and Coauthors, 2010: Record warming in the South Pacific and western Antarctica associated with the strong central-Pacific El Niño in 2009–10. *Geophys. Res. Lett.,* **37,** L19704, doi:10.1029/2010GL044865.

Lengaigne, M., E. Guilyardi, J. P. Boulanger, C. Menkes, P. Delecluse, and P. Inness, 2004: Triggering of El Niño by westerly wind events in a coupled general circulation model. *Climate Dyn.,* **23,** 601–620, doi:10.1007/s00382-004-0457-2.

L'Heureux, M. L., S. Lee, and B. Lyon, 2013: Recent multidecadal strengthening of the Walker circulation across the tropical Pacific. *Nat. Climate Change,* **3,** 571–576.

Lübbecke, J., and M. J. McPhaden, 2014: Assessing the twenty-first-century shift in ENSO variability in terms of the Bjerknes stability index. *J. Climate,* **27,** 2577–2587, doi:10.1175/JCLI-D-13-00438.1.

McGregor, S., A. Timmermann, M. H. England, O. Elison Timm, and A. T. Wittenberg, 2013: Inferred changes in El Niño-Southern Oscillation variance over the past six centuries. *Climate Past,* **9,** 2269–2284, doi:10.5194/cp-9-2269-2013.

McPhaden, M. J., 1999: Climate oscillations—Genesis and evolution of the 1997-98 El Niño. *Science,* **283,** 950–954, doi:10.1126/science.283.5404.950.

——, 2004: Evolution of the 2002–03 El Niño. *Bull. Amer. Meteor. Soc.,* **85,** 677–695, doi:10.1175/BAMS-85-5-677.

——, 2012: A 21st century shift in the relationship between ENSO SST and warm water volume anomalies. *Geophys. Res. Lett.,* **39,** L09706, doi:10.1029/2012GL051826.

Unauthenticated | Downloaded 12/18/20 10:22 AM UTC

——, and X. Yu, 1999: Equatorial waves and the 1997-98 El Niño. *Geophys. Res. Lett.,* **26,** 2961–2964, doi:10.1029/1999GL004901.

——, S. E. Zebiak, and M. H. Glantz, 2006: ENSO as an intriguing concept in Earth science. *Science,* **314,** 1740–1745, doi:10.1126/science.1132588.

——, T. Lee, and D. McClurg, 2011: El Niño and its relationship to changing background conditions in the tropical Pacific. *Geophys. Res. Lett.,* **38,** L15709, doi:10.1029/2011GL048275.

Moy, C. M., G. O. Seltzer, D. T. Rodbell, and D. M. Anderson, 2002: Variability of El Niño/Southern Oscillation activity at millennial timescales during the Holocene epoch. *Nature,* **420,** 162–165, doi:10.1038/nature01194.

Newman, M., M. A. Alexander, and J. D. Scott, 2011a: An empirical model of tropical ocean dynamics. *Climate Dyn.,* **37,** 1823–1841, doi:10.1007/s00382-011-1034-0.

——, S.-I. Shin, and M. A. Alexander, 2011b: Natural variation in ENSO flavors. *Geophys. Res. Lett.,* **38,** L14705, doi:10.1029/2011GL047658.

Ogata, T., S.-P. Xie, A. Wittenberg, and D.-Z. Sun, 2013: Interdecadal amplitude modulation of El Niño–Southern Oscillation and its impacts on tropical Pacific decadal variability. *J. Climate,* **26,** 7280–7297, doi:10.1175/JCLI-D-12-00415.1.

Penland, C., and P. D. Sardeshmukh, 1995: The optimal growth of tropical sea surface temperature anomalies. *J. Climate,* **8,** 1999–2024, doi:10.1175/1520-0442(1995)008<1999:TOGOTS>2.0.CO;2.

Qu, T., and J.-Y. Yu, 2014: ENSO indices from sea surface salinity observed by Aquarius and Argo. *J. Oceanogr.,* **70,** 367–375, doi:10.1007/s10872-014-0238-4.

Radenac, M.-H., F. Léger, A. Singh, and T. Delcroix, 2012: Sea surface chlorophyll signature in the tropical Pacific during eastern and central Pacific ENSO events. *J. Geophys. Res.,* **117,** C04007, doi:10.1029/2011JC007841.

Rasmusson, E. M., and T. H. Carpenter, 1982: Variations in tropical sea surface temperature and surface wind fields associated with the Southern Oscillation/El Niño. *Mon. Wea. Rev.,* **110,** 354–384, doi:10.1175/1520-0493(1982)110<0354:VITSST>2.0.CO;2.

Rayner, N. A., D. E. Parker, E. B. Horton, C. K. Folland, L. V. Alexander, D. P. Rowell, E. C. Kent, and A. Kaplan, 2003: Global analyses of sea surface temperature, sea ice, and night marine air temperature since the late nineteenth century. *J. Geophys. Res.,* **108,** 4407, doi:10.1029/2002JD002670.

Rodgers, K. B., P. Friederichs, and M. Latif, 2004: Tropical Pacific decadal variability and its relation to decadal modulations of ENSO. *J. Climate,* **17,** 3761–3774, doi:10.1175/1520-0442(2004)017<3761:TPDVAI>2.0.CO;2.

Ropelewski, C. F., and M. S. Halpert, 1987: Global and regional scale precipitation patterns associated with El Niño/Southern Oscillation. *Mon. Wea. Rev.,* **115,** 1606–1626, doi:10.1175/1520-0493(1987)115<1606:GARSPP>2.0.CO;2.

Sandeep, S., F. Stordal, P. D. Sardeshmukh, and G. P. Compo, 2014: Pacific Walker Circulation variability in coupled and uncoupled climate models. *Climate Dyn.,* **43,** 103-117, doi:10.1007/s00382-014-2135-3.

Schopf, P. S., and R. J. Burgman, 2006: A simple mechanism for ENSO residuals and asymmetry. *J. Climate,* **19,** 3167–3179, doi:10.1175/JCLI3765.1.

Shin, S.-I., P. D. Sardeshmukh, and R. S. Webb, 2010: Optimal tropical sea surface temperature forcing of North American drought. *J. Climate,* **23,** 3907–3917, doi:10.1175/2010JCLI3360.1.

Shukla, J., and D. A. Paolino, 1983: The Southern Oscillation and long-range forecasting of the summer monsoon rainfall over India. *Mon. Wea. Rev.,* **111,** 1830–1837, doi:10.1175/1520-0493(1983)111<1830:TSOALR>2.0.CO;2.

Singh, A., T. Delcroix, and S. Cravatte, 2011: Contrasting the flavors of El Niño and Southern Oscillation using sea surface salinity observations. *J. Geophys. Res.,* **116,** C06016, doi:10.1029/2010JC006862.

Smith, T. M., and R. W. Reynolds, 2004: Improved extended reconstruction of SST (1854–1997). *J. Climate,* **17,** 2466–2477, doi:10.1175/1520-0442(2004)017<2466:IEROS>2.0.CO;2.

Solomon, A., and M. Newman, 2012: Reconciling disparate twentieth-century Indo-Pacific ocean temperature trends in the instrumental record. *Nat. Climate Change,* **2,** 691–699, doi:10.1038/nclimate1591.

Stevenson, S., B. Fox-Kemper, M. Jochum, R. Neale, C. Deser, and G. Meehl, 2012: Will there be a significant change to El Niño in the twenty-first century? *J. Climate,* **25,** 2129–2145, doi:10.1175/JCLI-D-11-00252.1.

Sun, C., M. M. Rienecker, A. Rosati, M. Harrison, A. Wittenberg, C. L. Keppenne, J. P. Jacob, and R. M. Kovach, 2007: Comparison and sensitivity of ODASI ocean analyses in the tropical Pacific. *Mon. Wea. Rev.,* **135,** 2242–2264, doi:10.1175/MWR3405.1.

Sun, F., and J.-Y. Yu, 2009: A 10–15-yr modulation cycle of ENSO intensity. *J. Climate,* **22,** 1718–1735, doi:10.1175/2008JCLI2285.1.

Takahashi, K., A. Montecinos, K. Goubanova, and B. Dewitte, 2011: ENSO regimes: Reinterpreting the canonical and Modoki El Niño. *Geophys. Res. Lett.,* **38,** L10704, doi:10.1029/2011GL047364.

Unauthenticated | Downloaded 12/18/20 10:22 AM UTC

Taschetto, A., and M. H. England, 2009: El Niño Modoki impacts on Australian rainfall. *J. Climate,* **22,** 3167–3173, doi:10.1175/2008JCLI2589.1.

Tokinaga, H., S.-P. Xie, C. Deser, Y. Kosaka, and Y. M. Okumura, 2012a: Slowdown of the Walker circulation driven by tropical Indo-Pacific warming. *Nature,* **491,** 439–443, doi:10.1038/nature11576.

——, ——, A. Timmermann, S. McGregor, T. Ogata, H. Kubota, and Y. M. Okumura, 2012b: Regional patterns of tropical Indo-Pacific climate change: Evidence of the Walker circulation weakening. *J. Climate,* **25,** 1689–1710, doi:10.1175/JCLI-D-11-00263.1.

Trenberth, K. E., G. W. Branstator, D. Karoly, A. Kumar, N.-C. Lau, and C. Ropelewski, 1998: Progress during TOGA in understanding and modeling global teleconnections associated with tropical sea surface temperatures. *J. Geophys. Res.,* **103,** 14 291–14 324, doi:10.1029/97JC01444.

Turk, D., C. S. Meinen, D. Antoine, M. J. McPhaden, and M. R. Lewis, 2011: Implications of changing El Niño patterns for biological dynamics in the equatorial Pacific Ocean. *Geophys. Res. Lett.,* **38,** L23603, doi:10.1029/2011GL049674.

U.S. CLIVAR ENSO Diversity Working Group, 2013: U.S. CLIVAR ENSO Diversity Workshop report. U.S. CLIVAR Project Office Rep. 2013-1, 20 pp.

Vecchi, G. A., and A. T. Wittenberg, 2010: El Niño and our future climate: Where do we stand? *Wiley Interdiscip. Rev.: Climate Change,* **1,** 260–270.

——, ——, and A. Rosati, 2006: Reassessing the role of stochastic forcing in the 1997-8 El Niño. *Geophys. Res. Lett.,* **33,** L01706, doi:10.1029/2005GL024738.

Vimont, D., M. A. Alexander, and M. Newman, 2014: Optimal growth of central and east Pacific ENSO events. *Geophys. Res. Lett.,* **41,** 4027–4034, doi:10.1002/2014GL059997.

Wang, W., and H. H. Hendon, 2007: Sensitivity of Australian rainfall to inter–El Niño variations. *J. Climate,* **20,** 4211–4226, doi:10.1175/JCLI4228.1.

——, M. Chen, and A. Kumar, 2010: An assessment of the CFS real-time seasonal forecasts. *Wea. Forecasting,* **25,** 950–969, doi:10.1175/2010WAF2222345.1.

Wittenberg, A. T., 2004: Extended wind stress analyses for ENSO. *J. Climate,* **17,** 2526–2540, doi:10.1175/1520-0442(2004)017<2526:EWSAFE>2.0.CO;2.

——, 2009: Are historical records sufficient to constrain ENSO simulations? *Geophys. Res. Lett.,* **36,** L12702, doi:10.1029/2009GL038710.

——, A. Rosati, N.-C. Lau, and J. J. Ploshay, 2006: GFDL's CM2 global coupled climate models. Part III: Tropical Pacific climate and ENSO. *J. Climate,* **19,** 698–722, doi:10.1175/JCLI3631.1.

——, ——, T. L. Delworth, G. A. Vecchi, and F. Zeng, 2014: ENSO modulation: Is it decadally predictable? *J. Climate,* **27,** 2667–2681, doi:10.1175/JCLI-D-13-00577.1.

Xie, S.-P., 1999: A dynamic ocean–atmosphere model of the tropical Atlantic decadal variability. *J. Climate,* **12,** 64–70, doi:10.1175/1520-0442-12.1.64.

——, C. Deser, G. A. Vecchi, J. Ma, H. Teng, and A. T. Wittenberg, 2010: Global warming pattern formation: Sea surface temperature and rainfall. *J. Climate,* **23,** 966–986, doi:10.1175/2009JCLI3329.1.

Xue, Y., M. Chen, A. Kumar, Z.-Z. Hu, and W. Wang, 2013: Prediction skill and bias of tropical Pacific sea surface temperatures in the NCEP Climate Forecast System version 2. *J. Climate,* **26,** 5358–5378, doi:10.1175/JCLI-D-12-00600.1.

Yang, C., and B. S. Giese, 2013: El Niño Southern Oscillation in an ensemble ocean reanalysis and coupled climate models. *J. Geophys. Res. Oceans,* **118,** 4052–4071, doi:10.1002/jgrc.20284.

Yeh, S.-W., J.-S. Kug, B. Dewitte, M.-H. Kwon, B. Kirtman, and F.-F. Jin, 2009: El Niño in a changing climate. *Nature,* **461**, doi:10.1038/nature08316.

——, J.-S. Kug, and S.-I. An, 2014: Recent progress on two types of El Nino: Observations, dynamics, and future changes. *Asia-Pac. J. Atmos. Sci.,* **50,** 69–81.

Yu, J.-Y., and S. T. Kim, 2010: Identification of central-Pacific and eastern-Pacific types of ENSO in CMIP3 models. *Geophys. Res. Lett.,* **37,** L15705, doi:10.1029/2010GL044082.

——, and ——, 2011: Relationships between extratropical sea level pressure variations and the central Pacific and eastern Pacific types of ENSO. *J. Climate,* **24,** 708–720, doi:10.1175/2010JCLI3688.1.

——, and B. S. Giese, 2013: ENSO diversity in observations. *U.S. CLIVAR Variations,* Vol. 11, No. 2, U.S. CLIVAR Program, Washington, DC, 1–5.

——, H.-Y. Kao, and T. Lee, 2010: Subtropics-related interannual sea surface temperature variability in the equatorial central Pacific. *J. Climate,* **23,** 2869–2884, doi:10.1175/2010JCLI3171.1.

——, ——, ——, and S. T. Kim, 2011: Subsurface ocean temperature indices for Central-Pacific and Eastern-Pacific types of El Niño and La Niña events. *Theor. Appl. Climatol.,* **103,** 337–344, doi:10.1007/s00704-010-0307-6.

——, Y. Zou, S. T. Kim, and T. Lee, 2012: The changing impact of El Nino on US winter temperatures. *Geophys. Res. Lett.,* **39,** L15702, doi:10.1029/2012GL052483.

Zavala-Garay, J., C. Zhang, A. M. Moore, A. T. Wittenberg, M. J. Harrison, A. Rosati, J. Vialard, and R. Kleeman, 2008: Sensitivity of hybrid ENSO models

Unauthenticated | Downloaded 12/18/20 10:22 AM UTC

to unresolved atmospheric variability. *J. Climate,* **21,** 3704–3721, doi:10.1175/2007JCLI1188.1.

Zebiak, S. E., and M. A. Cane, 1987: A model El Niño–Southern Oscillation. *Mon. Wea. Rev.,* **115,** 2262–2278, doi:10.1175/1520-0493(1987)115<2262:AMENO>2.0.CO;2.

Zhang, H., A. Clement, and P. Di Nezio, 2014: The South Pacific meridional mode: A mechanism for ENSO-like variability. *J. Climate,* **27,** 769–783, doi:10.1175/JCLI-D-13-00082.1.

Zhang, S., M. J. Harrison, A. Rosati, and A. Wittenberg, 2007: System design and evaluation of coupled ensemble data assimilation for global oceanic climate studies. *Mon. Wea. Rev.,* **135,** 3541–3564, doi:10.1175/MWR3466.1.

Zheng, W., P. Braconnot, E. Guilyardi, U. Merkel, and Y. Yu, 2008: ENSO at 6ka and 21ka from ocean–atmosphere coupled model simulations. *Climate Dyn.,* **30,** 745–762, doi:10.1007/s00382-007-0320-3.

NEW FROM AMS BOOKS!

"A thoughtful analysis of actions that we need to take to reduce the impacts of extreme weather…a must-read for everyone with an interest in the weather and climate."

— FRANKLIN W. NUTTER,
President, Reinsurance Association of America

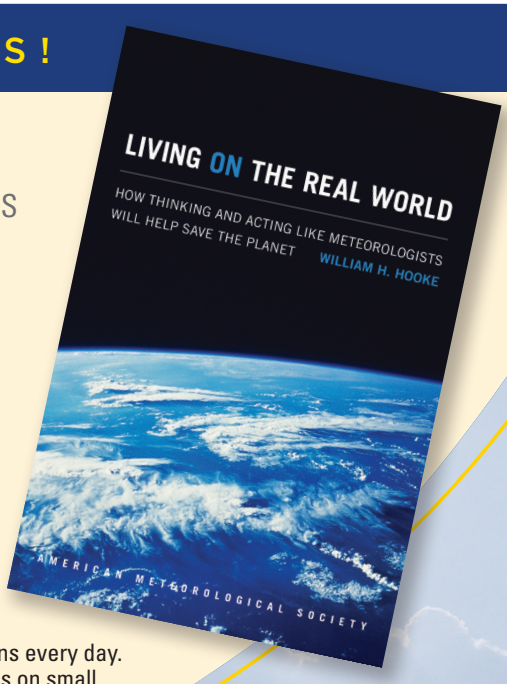

Living on the Real World:
How Thinking and Acting Like Meteorologists Will Help Save the Planet

WILLIAM H. HOOKE

Meteorologists sift through a deluge of information to make predictions every day. Instead of being overwhelmed by the data and possibilities, they focus on small bits of information while using frequent collaboration to make decisions. With climate change a reality, William H. Hooke suggests we look to the way meteorologists operate as a model for how we can solve the twenty-first century's most urgent environmental problems.

© 2014, PAPERBACK 978-1-935704-56-0
LIST $30 MEMBER $22

AMS BOOKS
RESEARCH APPLICATIONS HISTORY
www.ametsoc.org/amsbookstore

Unauthenticated | Downloaded 12/18/20 10:22 AM UTC